

Radiometric dating of sediment records in Kuwait's marine area

A. Aba · S. Uddin · M. Bahbahani ·
A. Al-Ghadban

Received: 8 December 2013 / Published online: 13 April 2014
© Akadémiai Kiadó, Budapest, Hungary 2014

Abstract Six sediment cores collected from the North-western Arabian/Persian Gulf have been radiometrically dated by ^{210}Pb . Three cores were collected from stations within the Kuwait Bay, and three others were collected from stations outside the bay. Two models have been used for ^{210}Pb dating of sediment cores, i.e. Constant Flux: Constant Sedimentation (CF:CS) Model and the Constant Rate of Supply (CRS) Model. The average rates were found to vary significantly between 0.16 and 1.00 cm y^{-1} for stations outside and within the bay respectively. The variability of the sedimentation rate was essentially physiographic characteristics and variable hydrodynamic condition. In this study, ^{137}Cs fallout radiotracer was also used to construct a realistic chronology. It was observed that the ^{137}Cs in the entire vertical profile has been continuously contributed by fluvial and atmospheric deposition.

Keywords Recent sediment deposition · ^{210}Pb dating · ^{137}Cs fallout · Kuwait Bay

Introduction

The Arabian Gulf (AG) is a shallow partly enclosed-marine water body, that is used for exporting, about one-third of

the world's oil produce. The Gulf also experiences excessive desalination activity, producing 11MCM d^{-1} of freshwater [1]. Several national and international programs have been executed to assess the pollution of the marine environment, as the result of the spilled and burned oil during the Gulf War in 1991 [2–6]. Moreover, steady increase in oil exports and establishment of new industries along the bay have exerted more stress on the fragile marine ecosystem of the Gulf. Most of the contaminants that get into the marine waters are bonded with the suspended solids. This emphasizes the need to have accurate estimation of the rate of sedimentation for reconstruction of pollution history, tracking the changing levels of these contaminants and tracing their pathways over the past decades for comprehensive environmental assessment. However, the previously work of Bem and Alzamel showed the applicability of using the radiometric dating techniques for dating the recent sediment deposition in the KB [7, 8].

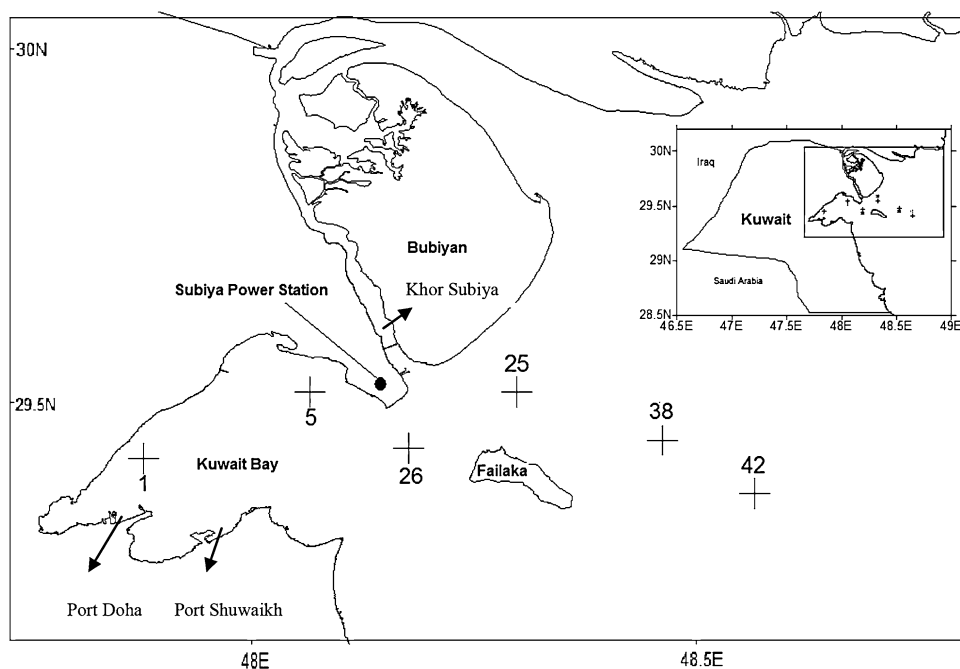
The use of the natural radionuclide ^{210}Pb for dating the recent sediment deposition in marine and freshwater environment has been well established since its first application by Goldberg in 1963 [9]. The ^{210}Pb half-life is 22.3 years covering a time scale spans 100–150 years. It provides a distinctive tool to estimate the sediment chronology in a water system as part of environmental pollution and climatic changes [10]. Such imperative radioactive tracers of fallout origin, similar to ^7Be , ^{210}Pb and ^{137}Cs , have been widely used to complement more conventional approaches for the estimation of sedimentation rate, the understanding of sediment transport and soil erosion [11–13].

Kuwait's territorial waters can be characterized into two distinct environmental milieus: the Kuwait Bay (KB) and the open sea. The KB is an embayment along a highly

A. Aba (✉)
Energy and Building Research Center, Kuwait Institute for
Scientific Research, P. O. Box 24885, Safat, Kuwait City 13109,
Kuwait
e-mail: aba.aziz@yahoo.com

S. Uddin · M. Bahbahani · A. Al-Ghadban
Environment and Life Science Center, Kuwait Institute for
Scientific Research, P. O. Box 24885, Safat, Kuwait City 13109,
Kuwait

Fig. 1 Site locations of the sediment core sampling stations



developed coastline in the south, and the open sea is shallow with highly turbid water in the north and clear deeper waters in the south. The six sediment cores have been collected from different micro-environments within the Northern Arabian Gulf. The rate of sedimentation is estimated in these cores which can be used to time integrate the change in pollution load that is observed in the Kuwait marine area using radiometric dating techniques. The average sedimentation rates were estimated using the ^{210}Pb technique along with the ^{137}Cs .

Materials and methods

Study area

The study area lies at the northwestern corner of the Northern Arabian Gulf (NAG), with a distinct physiographic unit the KB, which is an embayment covering about 720 km^2 area and has an average depth of about 10 m. The shoreline around KB hosts the major ports, namely Shuwaikh and Doha; three power and desalination plants, i.e., Doha east, Doha west and Subiya; and two wastewater treatment facilities at Jahra and Sula'biya, and over 17 storm water/emergency outfalls. All these inputs and the vast tidal flats in KB increase the susceptibility of acting as a repository for land-based pollution [14, 15]. The NGA area is heavily impacted by suspended particulate matter [16]. Excessive sedimentation is observed in the NGA as a result of heavy suspended particulate load consequent to destruction of mesopotomian marshes and due to long range transport of dust [2, 14, 15].

Sediment core sampling and preparation

Six sediment cores were collected from stations inside and outside the KB representing different environmental milieu (Fig. 1). $\text{KC}_{\text{Denmark}}$ Kajak Gravity sediment corer with 2 in diameter was used for core sample collection. The length of collected cores varied between 0.21 and 0.60 m. Each core was sliced at 2 cm interval and was dried overnight at $90\text{ }^\circ\text{C}$ before being ground. The dried sediment slices were sieved through a 0.5 mm sieve. A portion of the prepared sample was bottled in a 5 cm petri dish of 1 cm height. The petri dish was sealed and left for about a month to attain a secular equilibrium.

Gamma spectrometric measurement and analysis

Ultra low background Gamma-spectrometry system equipped with Canberra Broad Energy Ge series (BEGe) detectors was used to measure the gamma emissions of 5–3,000 keV with excellent low energy resolution (i.e., $\text{FWHM}@122\text{ keV}$ is 750 eV). The imperative characteristic of this spectroscopic system is the effective and appropriate shielding design that assists to determine natural and man-made radionuclides, including sources of low-energy gamma emitters, with very low detectable activity. The detector and the heavy shielding materials were manufactured from ultra low background materials. An active Veto shielding design was the most important part to effectively reduce the background levels. The detector efficiency was calibrated using an in-house calibration source, prepared by spiking the marine sediment with traceable gamma mixed standard solutions (QCYB-41

Table 1 Gamma spectral lines and the relative intensities used in the gamma spectrum analysis, yield uncertainty in brackets, (http://www.nucleide.org/DDEP_WG/DDEPdata.htm) accessed on January 2012

Radionuclide	Energy (keV)	Gamma yield (%)
²¹⁰ Pb	46.5	4.25 (4)
²²⁶ Ra	186.2	3.51 (6)
²¹⁴ Pb	295.2	18.41 (36)
	351.9	35.6 (7)
²¹⁴ Bi	609.3	45.49 (19)
	1120.3	14.91 (3)
	1764.5	15.31 (5)
¹³⁷ Cs	661.6	84.99 (20)

and QCYB-40) prepared by KDD Germany. This calibration source covered the energy ranges from 30 to 3 MeV. The correction for cascade summing was performed by the Genie 2000 analysis software.

The specific activities of ²¹⁴Pb, ²¹⁴Bi, ²²⁶Ra, ²¹⁰Pb and ¹³⁷Cs radionuclides were determined using the spectral lines presented in Table 1. It should be noted that the indirect determination of ²²⁶Ra activity was estimated, based on the weighted average activity for the strongest peaks of ²²⁶Ra radiogenic isotopes (²¹⁴Bi and ²¹⁴Pb). This arrangement eliminated the uncertainty caused by the interference of ²³⁵U gamma line when it was directly determined through the major gamma line (186.2 keV) of ²²⁶Ra. The minimum detectable activity for 30 g sample weight at 200,000 s counting was about 0.5 and 7.0 mBq g⁻¹ for each of ¹³⁷Cs and ²¹⁰Pb respectively.

²¹⁰Pb radiometric dating models

The theoretical basis of the ²¹⁰Pb radiometric dating techniques has been persistently described in detail in many research and technical notes [17–19]. ²¹⁰Pb dating method is based on the fact that ²¹⁰Pb incorporated into the sediments 22.3 years ago will be only one half as radioactive as when it was initially deposited. An important assumption to be considered when applying this method is that the deposition of the Lead-210 atmospheric fluxes over a specific area is constant since it is of a natural origin. Conspicuously, the total Lead-210 (²¹⁰Pb_{tot}) found in the sediment column has two sources, i.e., supported and unsupported Lead-210. The supported Lead-210 (²¹⁰Pb_{sup}) is in situ produced as a result of ²²⁶Ra decay presented in the sediment; while the unsupported or excess Lead-210 (²¹⁰Pb_{ex}) is a measure of Lead-210 atmospheric fallout incorporated into the sediment. The ²¹⁰Pb_{ex}, which is used in the theoretical ²¹⁰Pb dating models, is determined by subtracting the supported one from the total Lead-210 (i.e., ²¹⁰Pb_{ex} = ²¹⁰Pb_{tot} - ²¹⁰Pb_{sup}).

Consequently, the sediment accumulation rate can be determined by means the distribution of ²¹⁰Pb_{ex} in the sediment profile, which is governed by the general decay equation:

$$C(z) = C(0) e^{-\lambda\tau} \tag{1}$$

where C(z) is the ²¹⁰Pb_{ex} concentration in the sediment (Bq g⁻¹) at the depth z, C(0) is the initial unsupported ²¹⁰Pb_{ex} concentration at the time of the deposition (i.e., the ²¹⁰Pb concentration of the fresh deposition), λ is the decay constant of the Lead-210 which equals 0.03114 year⁻¹ and τ is the elapsed time between the Lead-210 deposition and its measurement date, which refers to the age of the sediment segment that can be derived from a suitable model [20].

When the relationship of the natural logarithm of the ²¹⁰Pb_{ex} concentration (Bq kg⁻¹) and the depth z (cm) shows a linear trend, the average sedimentation rate, S, can be calculated in a unit of (cm year⁻¹) using the linear regression parameters as follows:

$$S = -\frac{\lambda}{b} \tag{2}$$

where S, represents the average sedimentation rate (cm year⁻¹) of the sediment column over the constant slope b of the best regression line and λ is the decay constant of the ²¹⁰Pb. In this case the sedimentation rate is assumed constant along the entire sediment column and the method used is referred to the constant flux constant sedimentation rate (CF:CS) model [21]. This is legitimate only when the logarithmic ²¹⁰Pb_{ex} concentration profile demonstrates good statistical linearity verses depth z as indicated by the correlation coefficient R of the best regression line.

In general, the assumption is that the sedimentation rate is irregular or variable with time and hence the nonlinear model constant rate of supply (CRS) can be applied to calculate the age t of the sediment layer at depth x as follows [22]:

$$t_x = \frac{1}{\lambda} * \ln\left(\frac{A_{tot}}{A_x}\right) \tag{3}$$

where A_{tot} is the ²¹⁰Pb_{ex} total cumulative activity (inventory) of the entire sediment column (Bq m⁻²) and A_x is the cumulative activity of the ²¹⁰Pb_{ex} in the sediment column beneath depth x calculated by the following formulas:

$$A_x = \sum_{i=x}^{\infty} m_i C_i \tag{4}$$

$$A_{tot} = \sum_{i=1}^{\infty} m_i C_i \tag{5}$$

where m_i is the mass depth of a given layer i (g cm⁻²) and C_i is the concentration of the ²¹⁰Pb_{ex} in i layer (Bq g⁻¹).

Subsequently, the mass accumulation rate, r , of i sediment layer is calculated in a unit of mass per unit area ($\text{g cm}^{-2} \text{ year}^{-1}$) directly by the formula:

$$r_i = \frac{m_i}{t_i} \quad (6)$$

where m_i is the mass depth (g cm^{-2}) of the dated sediment layer i and t_i is the age of the sediment layer i . Consequently, the average mass accumulation rate of the sediment column \bar{r} can be calculated by the formula:

$$\bar{r} = \frac{m_{x2} - m_{x1}}{t_2 - t_1} \quad (7)$$

where m_{x1} and m_{x2} are the mass depths of the sediment layer x_1, x_2 corresponding to the ages t_1 and t_2 respectively.

It should be noted that the sediment dry bulk density ρ (g cm^{-3}) is usually used as a conversion factor to describe the mass accumulation rate ($\text{g cm}^{-2} \text{ year}^{-1}$) in a unit of (cm year^{-1}) when comparing the outputs of different sedimentation models as follows:

$$S(\text{cm y}^{-1}) = \bar{r}(\text{g cm}^{-2}\text{y}^{-1}) * \rho^{-1}(\text{cm}^{-3}\text{g}^{-1}) \quad (8)$$

Quality assurance

An in-house calibration source containing a mixture of marine sediments and a known quantity of the IAEA RGU-1 uranium ore reference material was used for quality control purposes [23]. Moreover, the reference material prepared by the International Atomic Energy Agency (IAEA) and coded as IAEA-477 [24] containing a known amount of ^{137}Cs , Uranium and Thorium radiogenic isotopes was filled with the same counting geometry, measured and analyzed in each batch of the sediment samples. The control chart and the analysis results of both quality control samples were employed to check the performance of the gamma spectrometry measurements and to maintain the quality of the analytical results.

Results and discussion

Application of ^{210}Pb models

The $^{210}\text{Pb}_{\text{ex}}$ activity was calculated in each segment of the sediment profile by means of the total ^{210}Pb specific activity determination. The relationship between the logarithm excess ^{210}Pb and the core depth was plotted and the best regression line was established. The adjusted R square (adj. R^2) value was used to describe the linearity of $^{210}\text{Pb}_{\text{ex}}$ distribution in depth. Besides the adj. R^2 indicator, which sometimes is not sufficient to express the linearity, the residual analysis output were used to evaluate the goodness of fit (i.e., the larger F value of the analysis of variance test,

the minimum residuals sum of squares and the best linear regression model). Based on that, the dating model, either CF:CS or CRS was selected to demonstrate the constant and irregular (variable) sedimentation rates respectively.

The distribution of the logarithmic excess concentration of $^{210}\text{Pb}_{\text{ex}}$ versus core depth showed a linear trend for stations 1, 38 and 42; where the adj. R^2 of the best regression lines were 0.84, 0.85 and 0.94 respectively; and hence the linear model CF:CS is fulfilled. In contrast, the adj. R^2 values of the best regression lines were less than 0.60 with relatively smaller F values for stations 5, 25 and 26, where the mode of sedimentation was probably irregular (variable), and hence the CRS model shows a better fit. Figure 2 shows the linear relationships between the logarithmic $^{210}\text{Pb}_{\text{ex}}$ and the core depth of the six stations.

Based on the previous explanation, an appropriate model was selected and the average sedimentation rate was calculated and presented in Table 2. It should be noted that the $^{210}\text{Pb}_{\text{ex}}$ profile of the core 26 showed a linear trend with good statistical parameters (i.e., Adj. $R^2 = 84$; F value = 47) only at the top of 15 cm while it was very poor (i.e., Adj. $R^2 = 27$; F value = 7) for the rest of the core length. Therefore, both models were applied to describe the sedimentation rate and to construct the chronology (i.e., CF:CS applied for the top 15 cm and CRS model applied for the entire column). However, applying the CRS model on the entire sediment column is still valid since the general assumption of sediment accumulation rate is variable. It is worth to mention that the uncertainty associated with the average sedimentation rate estimation of the linear model cores was based on the standard error of the best-weighted regression line that takes into account the error weight of the $^{210}\text{Pb}_{\text{ex}}$ determination. While the uncertainty associated with the CRS model involves propagating the sum of A_{tot}, A_x and ρ variances by the mathematical rules of error propagation. However, further sources of uncertainty influencing the calculation might be considered; for instance, the error related to sediment core slicing, compaction effect, sediment mixing due to bioturbation and sample preparation.

According to Table 2, the maximum average sedimentation rate reached the level of about $1.00 \text{ cm year}^{-1}$ for the stations situated within the bay; while it declined to a minimum of $0.16 \text{ cm year}^{-1}$ for the farthest station 42. Figure 3 shows the average sedimentation at each station from west to east. However, the significant variations of the sedimentation rate can be explained by the fact that the bay sector is characterized by a low current speed (low energy) [25], resulting in excessive sedimentation. In contrast, outside the bay is high energy environment that is not conducive for sedimentation. The rate of sedimentation at these stations decreases dramatically, least at station 42 ($0.16 \text{ cm year}^{-1}$). Although, the Total Suspended Solids (TSS) levels are higher in the area ($30\text{--}110 \text{ mg L}^{-1}$).

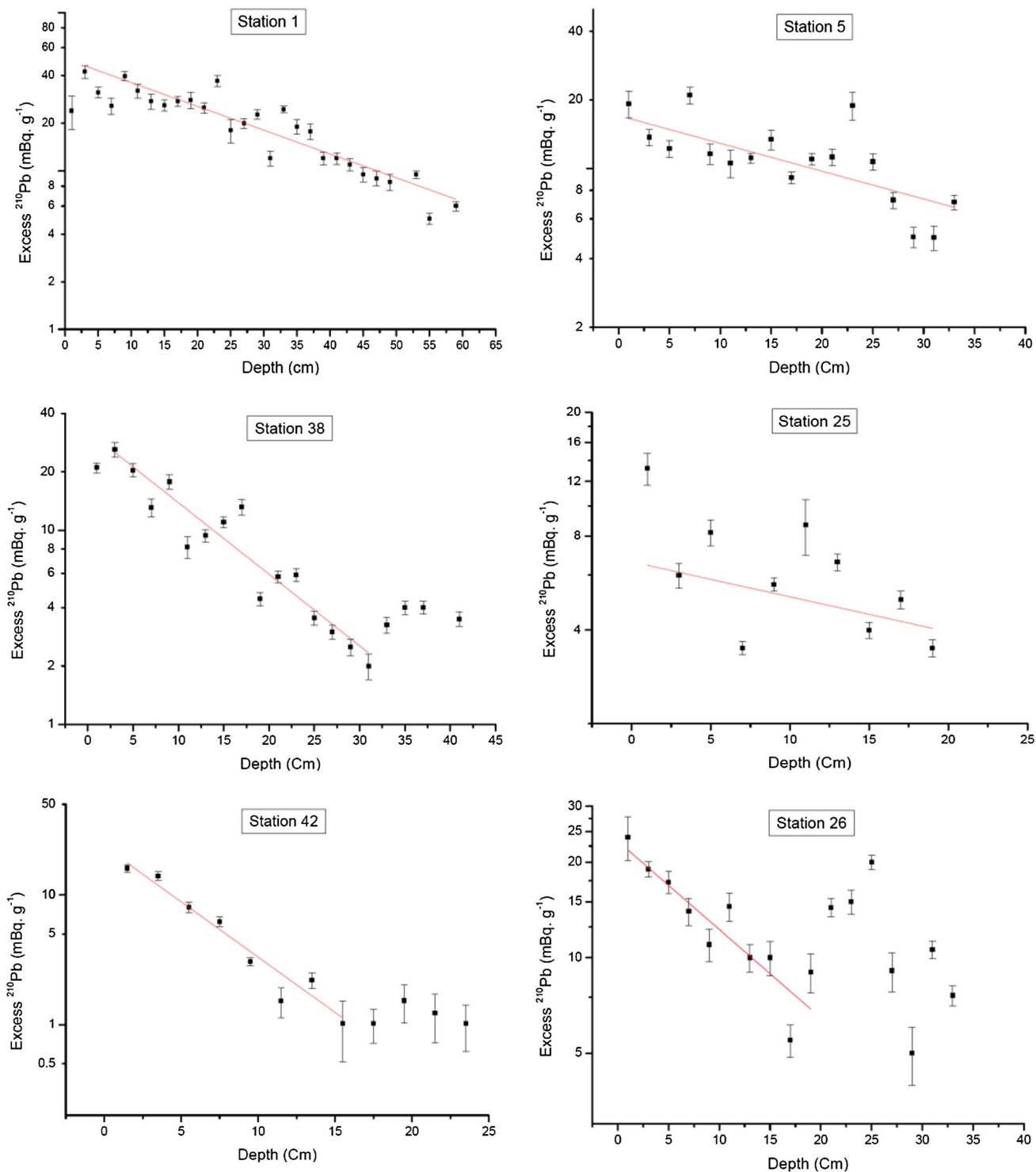


Fig. 2 The linear relationship between the logarithmic $^{210}\text{Pb}_{\text{ex}}$ and the core depth

The variability in sedimentation at stations 5, 25 and 26 can be attributed to varying hydrodynamics and currents, high turbidity and anthropogenic coastal activities, (possibly impact of the Subiya power plant construction in the early 1980s). However, the obtained results of the

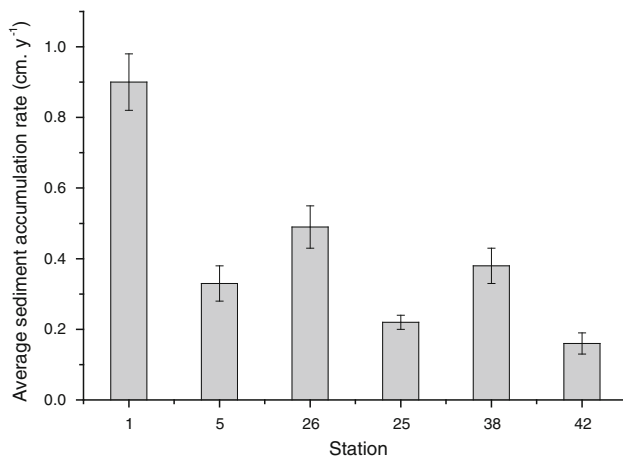
sedimentation rate of the station 5 ($0.33 \text{ cm year}^{-1}$) was within the range obtained earlier ($0.22\text{--}0.6 \text{ cm year}^{-1}$) [7].

The station No. 1 located at the west of KB is essentially a depositional basin with average depth of 4 m, characterized by excessively silty sediments and low energy

Table 2 Average sediment accumulation rates inside and outside the KB

Station	Average sedimentation rate (cm year ⁻¹) ± 2 SE*	Sediment bulk density (g cm ⁻³)	Sedimentation rate model	Core length (cm)	Adj. R ²	F value
1	0.90 ± 0.08	0.88	(CF:CS)	0–60	0.84	129
38	0.38 ± 0.05	1.00	(CF:CS)	0–28	0.85	71
42	0.16 ± 0.03	1.09	(CF:CS)	0–24	0.94	108
26 (1)	0.44 ± 0.06	0.85	(CF:CS)	0–15	0.84	47
26 (2)	0.49 ± 0.06	0.85	(CRS)	0–34	0.27	7
5	0.33 ± 0.05	0.95	(CRS)	0–34	0.54	20
25	0.22 ± 0.02	1.25	(CRS)	0–20	0.31	5

* Standard error

**Fig. 3** Average sediment accumulation rates; near to far from the coastal line

environment. The TSS concentration at this station are typically in range of 8–10 mg L⁻¹ but due to the counter clockwise current and low energy conditions, excessive deposition of sediments is observed in the area. The station 5 core collected from north east of KB is comparatively a higher energy environment. This station also receives direct inputs from the Subiya Power plant discharge, besides the trans-boundary sediment inputs. The TSS levels at and around this site typically is in 10–14 mg L⁻¹ range. Nevertheless, the sediment fraction is slightly coarser (silty-sand).

Stations 25 and 26 represent a very turbid environment with a TSS range of 30–110 mg L⁻¹ at different times characterized by sand size fraction. These are very high energy areas with shallow bathymetry, primarily influenced by the discharge from the Khor Subiya. The plume of the fluvial clastic extends until Failaka Island where the basin depth increases and sediment dispersion takes place.

Station 38 and 42 are typically offshore stations where the depth is >10 m. These areas are characterized by very low sedimentation rates. The bottom sediment types essentially are silty sand.

Verification of ²¹⁰Pb dating techniques by ¹³⁷Cs radiotracer

To confirm the accuracy of the selected sedimentation model, ¹³⁷Cs radionuclide was used as an independent time-stratigraphic marker. In general, ¹³⁷Cs deposition fluxes are well characterized and described by the hypothetical ¹³⁷Cs dispersion model in the northern and southern hemisphere [26]. According to the hypothetical model, ¹³⁷Cs peak derived from atmospheric-bomb testing occurred in the mid sixties and declined to the minimum in the late 1970s. Nevertheless, in some areas affected by the Chernobyl fallout, one more ¹³⁷Cs peak can be observed indicating the year 1986, when the Chernobyl accident occurred. It should be noted that in the ideal situation, two ¹³⁷Cs distinct peaks (one from the 1960s and one from mid 1980s) can be observed in the sediment profile.

Based on the previous information, the measured specific ¹³⁷Cs activities were converted to the activity per unit area (inventory) using Eq. 4 and plotted on the same graph of the theoretical ¹³⁷Cs derived bomb testing inventories of the northern hemisphere. It should be noted that the theoretical inventories were decay corrected to the sampling date, this arrangement made it easy to compare the theoretical and measured ¹³⁷Cs trends (Fig. 4). It is clear from Fig. 4 that incremental ¹³⁷Cs inventories are observed from beginning of the 1950s and reached a maximum between 1965 and 1980, and declined to a minimum in 1983. These observations are consistent with the theoretical ¹³⁷Cs data derived from atmospheric bomb-testing model, taken into consideration the high sedimentation rate. The slight increase in measured ¹³⁷Cs after 1986 could be associated with Chernobyl accident.

On the other hand, two distinct ¹³⁷Cs peaks were observed at station 38, located outside the bay. The measured ¹³⁷Cs pattern is consistent with the theoretical ¹³⁷Cs model when the uncertainty of the calculated age is taken (Fig. 4). The farthest station 42 showed that the measured ¹³⁷Cs increased around 1965, which could indicate the peak of the atmospheric bomb-test. The rate of sedimentation at

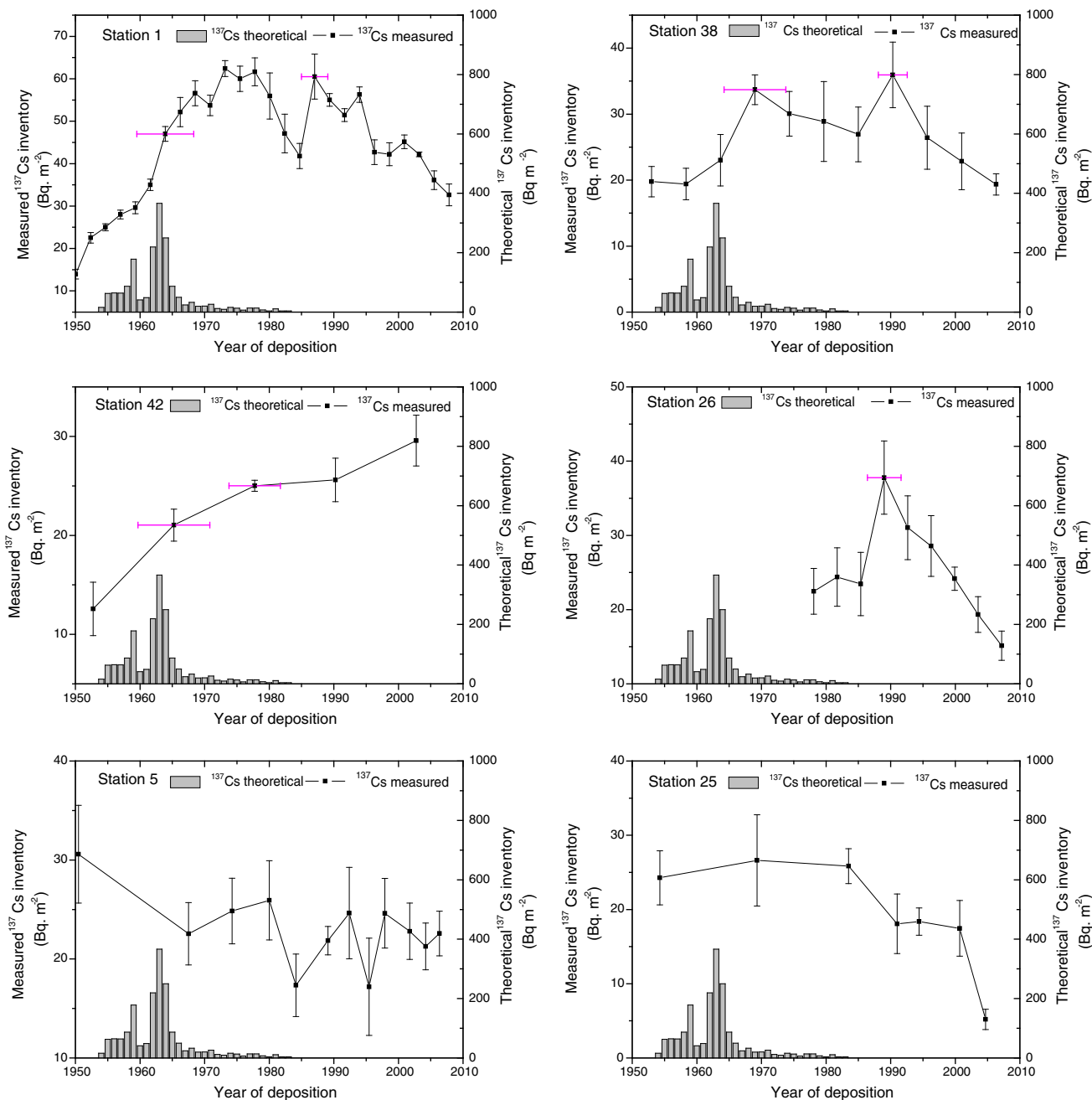


Fig. 4 The profiles of ¹³⁷Cs inventories of stations 1, 5, 26, 25, 38 and 42

this station is very low 0.16 cm year⁻¹ possibly representing the regional sedimentation pattern.

Finally, it can be concluded that the measured ¹³⁷Cs peak of the station 26 between 1982 and 1990 is related to the derived ¹³⁷Cs from Chernobyl accident. However, the first 1963 ¹³⁷Cs peak is not evident since the linear sedimentation model was only applicable for the top 15 cm of the core and the rest of the core showed sediment mixing. It should be noted that the measured ¹³⁷Cs in sediments of stations 5 and 25 have not shown any trend of ¹³⁷Cs

distribution in depth because of the sediment mixing and hence the sediment slices are disturbed, which resulted in an irregular ¹³⁷Cs pattern.

Conclusions

The average sedimentation using ²¹⁰Pb dating shows variable sedimentation between 0.16 and 1.00 cm year⁻¹ respectively for the cores situated outside and within the

KB. Irregularities in sediment depositions were observed in the top layers of the sediment core from stations within the KB. This is clearer in high deposition sites like station 1, where the average sedimentation rate reached about $1.00 \text{ cm year}^{-1}$. However, based on the measured ^{137}Cs , it was very hard to resolve ^{137}Cs peaks, either for the sixties or the eighties, since the Gulf area was less affected by the direct ^{137}Cs fallout. It is very likely that the measured ^{137}Cs is a result of constant influx of aeolian transport from Sub-Saharan desert, Turkey, Syria, Saudi Arabia, Iran and Iraq. Likelihood of fluvial trans-boundary sediment transport is also very high. It is very likely that the ^{137}Cs assimilated with dust is transported to the region at different times and thus a diffused ^{137}Cs activity is recorded across the entire vertical profile in marine sediments.

Unlike seen elsewhere ^{137}Cs cannot be used as a stratigraphic marker in northern Gulf, with the exception for areas of high sedimentation. Moreover, special care has to be taken when interpreting the ^{137}Cs pattern, due to the impact of the aeolian, fluvial sources, the bioturbation and the probability of ^{137}Cs diffusion that may redistribute its profile. Furthermore, sampling, sample preparation, and radioactivity measurement of low energy ^{210}Pb in addition to the measurement of very low level of ^{137}Cs radioactivity have to be given great care to apply the method successfully.

Acknowledgments The authors wish to thank the Kuwait Foundation for the Advancements of Sciences (KFAS) for their financial support. The authors also wish to express their gratitude to Dr. Najj M. Al-Mutairi, Director General for his support. The authors deeply thank Anfal Ismaeel for her contribution in sample preparation and measurements. Special thanks go to Dr. M. Quine, the senior researcher at KISR for his valuable comments and discussion.

References

- Uddin S, Ghabban ANA, Khabbaz A (2011) Localized hyper saline waters in Arabian Gulf from desalination activity an example from South Kuwait. *Environ Monit Assess* 181(1–4):587–594
- Al Ghabban A, Uddin S, Aba A, Behbehani M (2010) Measurement and assessment of radionuclide concentrations in the coastal marine environment. *Kuwait Institute for Scientific Research (KISR)* 9946:1–25
- Al-Abdali F, Massoud M, Al-Ghabban A (1996) Bottom sediments of the Arabian Gulf III. Trace metal contents as indicators of pollution and implications for the effect and fate of the Kuwait oil slick. *Environ Pollut* 23:285–301
- Al-Ghabban A, Massoud M, Abdali F (1996) Bottom sediments of the Arabian Gulf: sedimentological characteristics. *Kuwait J Sci Eng* 23:71–88
- Massoud M, Al-Abdali F, Al-Ghabban A, Al-Sarawi M (1996) Bottom sediments of the Arabian Gulf II. TPH and TOC contents as indicators of oil pollution and implications for the effect and fate of the Kuwait oil slick. *Environ Pollut* 93(3):271–284
- Metwally M, Al-Muzaini S, Jacob P, Bahloul M, Urushigawa Y, Sato S, Matsumura A (1997) Petroleum hydrocarbons and related heavy metals in the near-shore marine sediments of Kuwait. *Environ Int* 23:115–121
- Al-Zamel A, Bou-Rabee F, Olszewski M, Bem H (2005) Natural radionuclides and ^{137}Cs activity concentration in the bottom sediment cores from Kuwait Bay. *J Radioanal Nucl* 266:269–276
- Bem H (2006) Determination of the sediment deposition rates in the Kuwait Bay using ^{137}Cs and ^{210}Pb . *Nukleonika* 51(Suppl 2):S39–S44
- Goldberg ED (1963) The sea: ideas and observations on progress in the study of the seas. In: Hill, M.N. (Ed) *The oceans as a chemical system*. vol 2. The composition of seawater and Comparative and descriptive oceanography. Wiley, New York
- Appleby P, Jones V, Ellis-Evans J (1995) Radiometric dating of lake sediments from Signy Island (maritime Antarctic): evidence of recent climatic change. *J Paleolimnol* 13:179–191
- Walling D, He Q (1999) Using fallout lead-210 measurements to estimate soil erosion on cultivated land. *Soil Sci Soc Am J* 63:1404–1412
- Walling D, He Q, Blake W (1999) Use of ^7Be and ^{137}Cs measurements to document short-and medium-term rates of water-induced soil erosion on agricultural land. *Water Resour Res* 35:3865–3874
- Zapata F, Garcia-Agudo E, Ritchie JC, Appleby P (2003) Chapter 1: Introduction. In: Zapata F (ed). Springer, Amsterdam, pp 1–13
- Al-Ghabban A, Uddin S, Beg M, Al-Dousari A, Gevao B, Al-Yamani F (2008) Ecological consequences of river manipulations and drainage of Mesopotamian marshes on the Arabian Gulf ecosystem: investigations on changes in sedimentology and environmental quality, with special reference to Kuwait Bay. *Kuwait Institute for Scientific Research (KISR)* 9362: 1–141
- Uddin S, Al-Ghabban A, Gevao B, Al-Shamroukh D, Al-Khabbaz A (2012) Estimation of suspended particulate matter in Gulf using MODIS data. *Aquat Ecosyst Health Manage* 15(S1): 41–44
- Neelamani S, Uddin S (2013) Erosion and Accretion Index for Kuwaiti Coast. *Int J Environ Res* 7(3):679–684
- Corcoran MK (2007) Geomorphic identification and verification of recent sedimentation patterns in the Woonasquatucket River, North Providence, Rhode Island <http://oai.dtic.mil/oai/oai?verb=getRecord&metadataPrefix=html&identifier=ADA464865>. Accessed 21 Nov 2013
- Crickmore M, Tazoli G, Appleby P, Oldfield F (1990) The use of nuclear techniques in sediment transport and sedimentation problems. UNESCO
- Appleby PG (2002) Chronostratigraphic techniques in recent sediments. In: Last W, Smol J (eds). Springer, Netherlands, pp 171–203
- Appleby P, Oldfield F (1992) Application of lead-210 to sedimentation studies. *Uranium-series disequilibrium: applications to earth, marine and environmental sciences*. Clarendon Press, Oxford, pp 731–778
- Oldfield F, Appleby P (1984) Empirical testing of ^{210}Pb -dating models for lake sediments. In: Haworth EY, Lund JWG (eds) University of Minnesota. Minneapolis, Mn, pp 93–124
- Appleby P, Oldfield F (1978) the calculation of lead-210 dates assuming a constant rate of supply of unsupported ^{210}Pb to the sediment. *Catena* 5(1):1–8
- Aba A, Ismaeel A (2013) Preparation of in-house calibration source for the use in radioactivity analysis of the environmental samples: consideration of homogeneity. *J Radioanal Nucl* 295(1): 1–10

24. Shkhashiro A, Tarjan S, Ceccatelli A, Kis-Benedek G, Betti M (2012) IAEA-447: a new certified reference material for environmental radioactivity measurements. *Appl Radiat Isot*. doi:[10.1016/j.apradiso.2012.01.024](https://doi.org/10.1016/j.apradiso.2012.01.024)
25. Al-Ghadban A (1990) Holocene sediments in a shallow bay, southern coast of Kuwait, Arabian Gulf. *Mar Geol* 92(3–4):237–254
26. UNSCEAR (2000) Sources and effects of ionizing radiation: Sources Annex C: exposures to the public from man-made sources of radiation